TEMPERATURE-COUPLED RHYTHM GENERATION AND AVERSIVE CUE DISCRIMINATION IN THE MOUSE THALAMUS

THESIS BOOKLET

KINGA KOCSIS

ADVISORS:

ISTVÁN ULBERT, MD, DSC
FERENC MÁTYÁS, PHD

PÁZMÁNY PÉTER CATHOLIC UNIVERSITY
FACULTY OF INFORMATION TECHNOLOGY AND BIONICS
ROSKA TAMÁS DOCTORAL SCHOOL OF SCIENCES AND TECHNOLOGY

BUDAPEST, 2021.

My doctoral research is dedicated to add to the growing body of research that features the thalamus beyond a passive messenger role. It is highlighted as a dynamic gateway where various afferents and physiological factors can alter adaptive thalamic communication with telencephalic structures, thus, ultimately learning, and behavioral plasticity itself.

My studies hereby focused on a primary thalamic mechanism, sleep spindle generation in the ventral posteromedial (VPM), and on a non-primary, affective sensory function in the posterior intralaminar (PIL) and suprageniculate (SG) thalamic nuclei.

PART 1 Study of temperature-coupled dynamics of sleep spindles

1.1. Motivation and aims of the study

Whereas sleep propensity and quality are highly dependent on thermal conditions, and sleep regulation is coupled to thermoregulation (Krauchi & Deboer, 2010), the temperature dependence of the underlying neuronal network activity of sleep is sporadically addressed.

Studies in mammalian species have shown that there are multiple changes in body and brain temperature even during a single sleep session. NREM (non-rapid eye movement) sleep is associated with decreased brain and body temperature, but during REM, brain temperature shows a paradoxical increase in many terrestrial species (Kawamura & Sawyer, 1965; Kovalzon, 1973; Lyamin *et al.*, 2018). Furthermore, core body temperature can vary across individuals (Sund-Levander *et al.*, 2002) or with changes in ambient temperature (Alföldi *et al.*, 1990).

It is well-known that temperature affects the rate of biological processes; despite constant redistribution of cerebral heat, neuronal activity is also a function of temperature. Changes in body temperature have the potential to entrain brain state fluctuations (Whitten *et al.*, 2009); a brain temperature change of 1 °C is sufficient to shift EEG frequencies above 10 Hz by 1 Hz (Deboer & Tobler, 1995). Temperature-dependent changes in brain oscillations that reflect the activity of synchronized neural populations, point towards deeper consequences of thermal change in network function.

Amongst thalamocortical oscillations, sleep spindles (7-15 Hz frequency, 1-3 s length) are transient rhythmic activities during the early stages of sleep. They are generated by the mutual rhythmic interaction of excitatory thalamocortical (TC) projection neurons and inhibitory thalamic reticular (Rt) neurons, that in turn entrains cortical network activity (Steriade *et al.*, 1985). Spindles have been the subject of many studies on sleep quality, memory encoding and mental health. At the same time, these transient oscillations are very susceptible to thermal changes of the mammalian body. Frequency of spindle oscillations strongly co-varies with physiological body temperature changes reoccurring across the menstrual cycle (Driver *et al.*, 1996). Spindle activity also shows circadian modulation with a peak density at habitual sleep onset, time-locked to the

maximal decrease in core temperature (Dijk & Czeisler, 1995). Thus, it is essential to further study how spindle dynamics are affected by body and brain temperature variations.

Several poikilothermic animals employ compensatory mechanisms to make their neural oscillators robust to thermally challenging environments (Tang *et al.*, 2012). Whether a similar mechanism exists in the mammalian thalamocortical system remains to be elucidated.

In this part of my studies, I sought to examine the relationship between sleep spindle oscillations and changing core/brain temperatures.

- I investigated the changes in spindle oscillations while manipulating and measuring core as well as selectively brain temperature (**Aim Ia**);
- I studied how this rhythmic neuronal activity relates to the microarchitecture of baseline brain temperature variations (**Aim Ib**).

1.2. Experimental approaches

Ia. The first aim was to investigate the temperature dependence of spindle oscillations in mice with minimal interference from global thermoregulation. To this end, we employed urethane anesthesia, which is known to impair thermoregulatory processes (Malkinson *et al.*, 1988), yet it closely mimics natural sleep (Clement *et al.*, 2008). This way, core body temperature can be manipulated by external heating within quasi-physiological boundaries.

Linear 16-channel NeuroNexus (Ann Arbor, MI, USA) silicon probes were used to record broadband activity from the ventral posteromedial thalamic nucleus (VPM) and the primary somatosensory cortex of anesthetized C57BL/6 male mice (n=8) (**Figure 1.3.1.1./a**). The animals' core body temperature was varied between 34 and 39 °C (**Figure 1.3.1.1./b**). To simultaneously measure brain temperature and ongoing VPM activity, we used the thermoelectrode developed in a collaboration with our lab (Fekete *et al.*, 2017). This probe has regular recording sites for unit activity, as well as a temperature sensitive meander, capable of measuring the temperature of the surrounding tissue with an absolute precision of <0.2 °C (relative precision <0.002 °C). Recordings were made with 16-channel Intan RHD2132 amplifiers, connected to an RHD2000 evaluation board (Intan Technologies Llc.). Brain temperature was measured upon calibration and measurement of the resistance of the platinum filament in the thermoelectrode (Fekete et al., 2017) with a Keithley 6221 precision current generator and a Keithley 2000MM multimeter (Keithley Instruments Inc). All signals were sampled at 20 kHz, except for brain temperature, sampled at 5 Hz. The electrocardiogram (ECG) as well as rectal and brain temperature were simultaneously recorded with the local field potential (LFP) by using the analog inputs of the RHD2000 system.

Sleep spindles were detected semi-automatically form the smoothed and filtered (8-20 Hz), downsampled (1 kHz) multi-unit activity (MUA) from both the thalamus and the cortex. The frequency of spindles was calculated from the average interval between the detected cycle peaks.

Spindle prevalence was calculated in 2-minute time bins. Temperature value measured at the start of the respective spindle was considered for analysis. To give the common measure for the temperature dependence of spindle frequency, Q_{10} was calculated.

Sigma power was determined from the multi-unit activity (filtered for 6-18 Hz). Heart rate was calculated from the detected R-waves of the ECG signal. In the case of the infraslow oscillations, all respective signals were smoothed with a 10 s window and then downsampled while brain temperature was interpolated to 10 Hz. Sigma band and MUA were normalized to their means.

Ib. Brain temperature closely followed changes in core temperature across all animals (**Figure 1.3.1.1./c**), brain temperature being lower by 2-3 °C, as expected in small animals under anesthesia (LaManna *et al.*, 1989). However, we used the platinum filament in the thermoelectrode to selectively heat up adjacent brain tissue by increasing the current in the 4-wire resistance measurement setup (Fekete *et al.*, 2017).

In these experiments, the thermoelectrode was inserted into the VPM (n=7), while the animals' core temperature was kept constant at ~36 °C. In addition, a linear electrode was placed in the contralateral VPM for control recording (**Figure 1.3.1.2./a**). We employed cycles of 2 minutes of measurement current (1 mA) and 2 minutes of heating current (4, 6, 8 mA) (**Figure 1.3.1.2./b**). The latter increased tissue temperature in a gradual fashion up to 3 °C, and this heating effect remained relatively local. The direct current passing the probe did not stimulate the unit activity electrically (Fekete *et al.*, 2017), did not disrupt the recurrence of spindling epochs, and did not impair spindles (**Figure 1.3.1.2./c**).

All analysis was done with custom-written MATLAB (MathWorks) codes.

1.3. New scientific contributions

1.3.1. **Thesis Ia**

With combined extracellular electrophysiological, core body and brain temperature recordings, I showed in urethane-anesthetized mice that sleep spindle frequency increases, length decreases with core and consequently with brain temperature. Local tissue warming reproduces the effects only on the heated spot, suggesting a local biophysical mechanism.

Related journal publication: [J1]

I participated in the conception, design and methodological foundation of the experiments, the acquisition, analysis and interpretation of the acute electrophysiological and temperature data. I took part in the drafting and revision of the related section of the manuscript.

Related conference presentations: [C1]-[C6]

Though temperature dependence of EEG rhythms has been described before, this is the first *in vivo* study to integrate LFP and MUA recordings with brain temperature measurements on a single device, as well as use local heating to explore the underlying mechanism.

Spindle frequency and duration were consistently and inversely modulated by both core and brain temperature in the majority of animals, both in the thalamus and the cortex (**Figure 1.3.1.1./d-e**). Since brain temperature changes followed body temperature, the examined parameters also correlated with core body temperature (**Figure 1.3.1.1./f**). The modulation of spindle frequency was given as Q_{10}, which expresses the rate of change when the temperature increases by 10 °C. We measured a median value of 2.44 for the thalamic spindles (**Figure 1.3.1.1./g**). This fits in the range given for the temperature dependence of neural oscillations, 2.3-2.7 (Deboer & Tobler, 1995), suggesting that this rate may be a general phenomenon in the central nervous system.

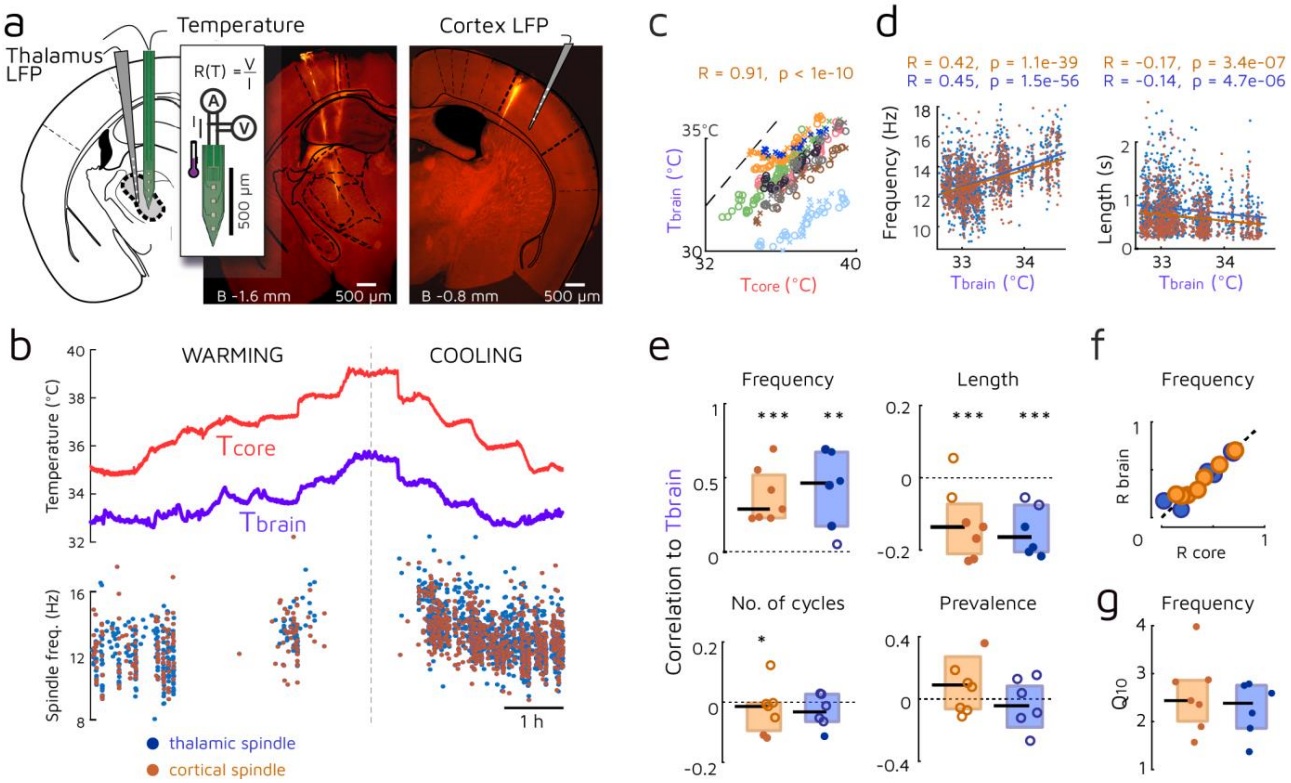

Figure 1.3.1.1. Sleep spindle frequency and length correlate with brain and core body temperature.

a/ Recording of LFP, MUA and temperature from the VPM thalamic nucleus with a linear 16-channel probe, and with our custom-designed thermoelectrode (left DiI tracks). Temperature was measured by four-wire resistance measurement of the platinum filament in the thermoelectrode calibrated to 1mA current (inset). Control LFP recordings (right) with a linear 16-channel probe from the contralateral primary somatosensory cortex (shown) or VPM. **b/** Example of core body and brain temperature under warming and cooling protocols. Spindle frequency is modulated by both core and brain temperature both in the thalamus and the cortex. **c/** Both under warming and cooling protocols, core body temperature correlates with brain temperature across multiple animals (n=8 mice). **d/** Both thalamic and cortical spindle frequency (left) correlates with brain temperature in the example experiment shown in **b**. Length of spindles has an inverse correlation with brain temperature (right). **e/** Pooled correlation coefficients show that temperature dependence of spindle frequency is a significant effect across animals. Spindle duration is negatively modulated, while the number of spindle cycles and spindle prevalence do not depend on brain temperature. *t-test,* ***p<0.005, **p<0.01, *p<0.05). **f/** Modulation of spindle frequency is consistent across core and brain temperature (dotted line is unity). **g/** Median Q_{10} value of spindle frequency perfectly fits the biological range of 2-3.

Published in (Csernai & Borbély & Kocsis et al., 2019) Figure 1./A, D-H.

As seen in **Figure 1.3.1.2./d**, local application of increasing heating currents (4, 6 and 8 mA) produced a progressive increase in local spindle frequency as compared to the control periods. Notably, there was an adverse effect on the contralateral side, which might arise from increased hypothalamic temperature sensation or an altered blood perfusion, but it was a magnitude smaller and non-significant in the pooled data compared to the ipsilateral effect of tissue heating. Duration of the spindles also decreased significantly by 25.7+/-3.8 % in the case of 8 mA heating. These results imply that the temperature dependence of spindle frequency is largely due to local biophysical processes instead of global modulatory mechanisms.

The frequency range of spindles is suited for inducing LTP in cortical circuits (Rosanova & Ulrich, 2005), so any change in the frequency of this oscillation is likely to affect synaptic potentiation. In case spindles contribute to temporal binding, creating a temporal window for synchronous firing, spindle frequency also has a crucial role in it. An alternative would be that the information carried by spindles is determined by the different cohorts of neurons involved in each cycle. Here, the increase in spindle frequency was compensated by a smaller decrease in spindle duration, which may reflect the robustness of information encoding in spindles with regard to brain temperature.

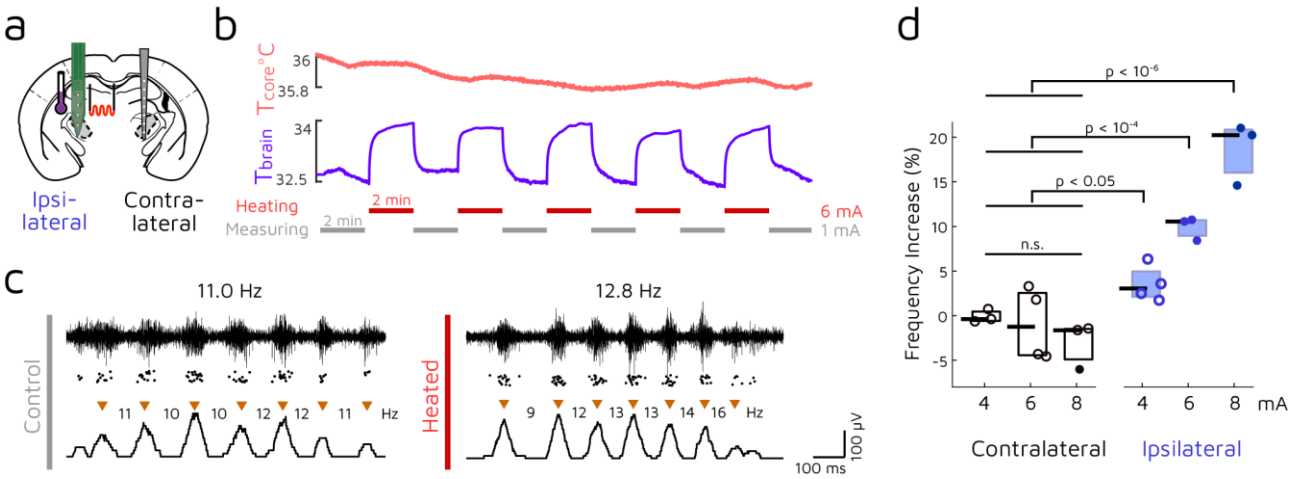

Figure 1.3.1.2: Temperature influences sleep spindles by a local mechanism.

a/ In one hemisphere, the VPM/VPL thalamus was locally heated with the thermoelectrode, while neural activity was recorded both locally and in the contralateral thalamus (n=7 mice). Temperature of the ipsilateral surrounding tissue was also monitored with a thermistor. ***b/*** The ipsilateral thalamus was heated in 2 min on / 2 min off cycles. ***c/*** Representative examples of thalamic spindles without and during heating (black trace: high-pass filtered recording, dots: detected multi-unit, triangles: detected spindle cycles above the smoothed MUA). Note that unit activity and spindle structure are undisturbed. ***d/*** Pooled results of 4 animals show a gradual effect in thalamic spindle frequencies with an increasing heating current (open circles: non-significant effect, filled circles: significant effect with *two-sample t-tests* at p<0.01; pooled significance: *Mann-Whitney-Wilcoxon test*).

Published in (Csernai & Borbély & Kocsis et al., 2019) Figure 2./A, C, D, F.

1.3.2. **Thesis Ib**

I showed in urethane-anesthetized mice that baseline microfluctuations in brain temperature are associated with sleep spindle oscillations. Besides the larger, REM-like periodic elevation of brain temperature, smaller temperature variations correspond to the infraslow oscillation (~0.02 Hz).

Related journal publication: [J1]

I performed the first analyses and gathered the preliminary evidence for the baseline microfluctuations in brain temperature, which are marked by the comodulation of brain temperature and sleep spindles. I took part in the methodological foundation of the analysis, as well as the interpretation of the acute electrophysiological and temperature data. I took part in the drafting and revision of the related section of the manuscript.

Related conference presentations: [C1], [C2], [C5], [C6]

Besides brain temperature influencing neural oscillations, spontaneous alterations of brain states may alter brain temperature, too. Beyond the gross changes induced by heating and cooling, brain temperature also shows periodic baseline fluctuations on a scale smaller by an order of magnitude (**Figure 1.3.2./a**). These fluctuations are superimposed on, and appear irrespectively of the absolute brain temperature, and spindling periods are associated with these elevated brain temperature epochs (see also in (Fekete *et al.*, 2017).

Larger elevations (Type I., order of 10^{-1} °C) can correspond to REM activity, observed in certain mammals (Hayward & Baker, 1969), as REM might serve a transient recovery from a reduced metabolism and brain temperature brought about by bihemispheric NREM sleep (Lyamin *et al.*, 2018). On a smaller scale (Type II., order of 10^{-2} °C), brain temperature fluctuates in synchrony with the infraslow oscillation (0.02 Hz) (**Figure 1.3.2./b**) that involves sigma power, individual spindle events as well as heart rate. Importantly, thalamic spindling is shown to forego brain temperature fluctuation (**Figure 1.3.2./c**).

The latter finding has been reviewed by (Fernandez & Lüthi, 2020), highlighting the clustering of sleep spindles on the 0.02 Hz infraslow time scale, which follows the alternation of fragile and continuous NREM periods. The infraslow oscillation has been previously observed in rodents, carnivores and humans (Steriade *et al.*, 1993; Lőrincz *et al.*, 2009; Lecci *et al.*, 2017), modulating LFP sigma band as well as heart rate (Lecci *et al.*, 2017), pupil size (Blasiak *et al.*, 2013), and fMRI BOLD signal (Mantini *et al.*, 2007). Its expression in TC population activity can originate from local astrocytes (Lőrincz *et al.*, 2009), a subpopulation of which has been shown to generate pacemaker calcium oscillations at ~0.019 Hz (Parri & Crunelli, 2001).

What can be the cause of the temperature microfluctuations? Physiological and pathological temperature changes of the brain can be directly derived from the changes of local metabolism, cerebral blood perfusion, and blood temperature (Hayward & Baker, 1969; Wang *et al.*, 2014). In our case, temperature elevations were correlated with increased multi-unit activity, which, together

with local astrocyte signaling, may increase temperature directly, or via enhancing the local blood flow.

Overall, these oscillatory phenomena point to a tight temporal coupling of metabolic and hemodynamic changes with neuronal network mechanisms, which are co-modulated on multiple time scales.

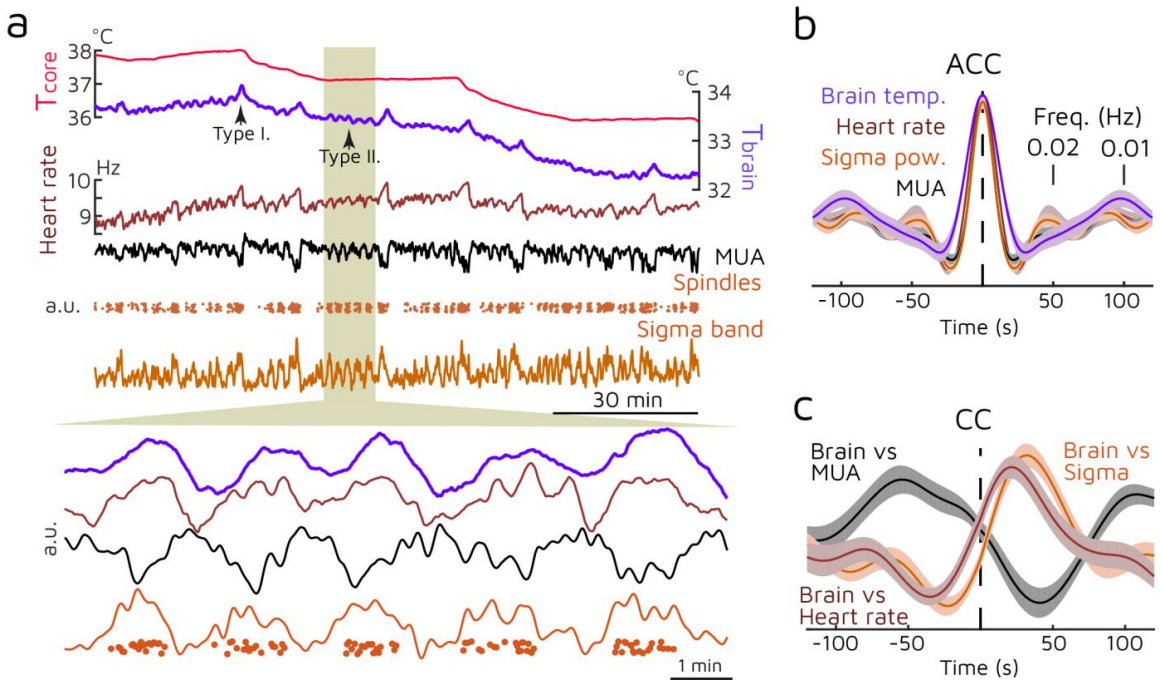

Figure 1.3.2. Microfluctuations in brain temperature accompany spindling epochs under urethane anesthesia.

a/ Example recording where microfluctuations of brain temperature, heart rate and spindle (sigma) power appear to be in synchrony. On a finer time scale (zoom-in), sigma power, heart rate and brain temperature can be seen to oscillate together with an apparent temporal order between them. **b*/*** Averaged autocorrelograms of pooled urethane data show that these microfluctuations are in the infraslow frequency range (~0.02 Hz). **c*/*** Pooled cross-correlations (brain temperature vs. other) show that spindling and heart rate forego brain temperature fluctuation, while general thalamic MUA lags behind. Values on **b** and **c** are normalized.

Published in (Csernai & Borbély & Kocsis et al., 2019) Figure 4./A-D.

1.3.3. **Outlook: potential for the study**

Robustness in neuronal rhythm generation and sleep can be highly dependent on external and internal thermal conditions. This is an adaptive challenge for many wild species exposed to a changing climate, but also for humans whose behavioral thermoregulation is impaired, such as the disabled and the elder (Collins *et al.*, 1981) as well as those suffering from neurological illnesses.

Peak density of spindles was measured during the maximal decrease in core temperature (Dijk & Czeisler, 1995), and I also observed increased spindle activity in the decaying phase of core and brain temperature modulation, with the oscillations becoming sparse with a rising temperature (see **Figure 1.3.1.1./b**). This observation also suggests that higher body temperatures (e.g., fever) can disrupt neural oscillations.

There is an epidemic of sleep disturbances, which are often diagnosed as comorbidity in many diseases and psychiatric disorders. Studying the interdependence of core/peripheral body temperature, neuronal network activity and blood perfusion can further our understanding on many debilitating conditions and on their possible treatments. Interventions which target the intensity, area, duration and timing of body and brain temperature fluctuations can be crucial in improving sleep quality in a large population (Van Someren, 2000, 2004; Raymann *et al.*, 2008).

1.4. Relevant publications

1.4.1. **Peer-reviewed articles**

Publication supporting the theses

[J1] Csernai M*, Borbély S*, Kocsis K*, Burka D, Fekete Z, Balogh V, Káli Sz, Emri Zs, Barthó P (2019): Dynamics of sleep oscillations is coupled to brain temperature on multiple scales. *Journal of Physiology, 597(15),* pp. 4069-4086. https://doi.org/10.1113/JP277664

*shared first authorship

Other relevant publications

[J2] Fekete Z, Csernai M, Kocsis K, Horváth ÁC, Pongrácz A, Barthó P (2017): Simultaneous in vivo recording of local brain temperature and electrophysiological signals with a novel neural probe. *Journal of Neural Engineering, 14(3)*. 034001 https://doi.org/10.1088/1741-2552/aa60b1

[J3] Horváth ÁC, Kocsis K, Csernai M, Barthó P, Fekete Z (2016): A Novel Neural Probe for Simultaneous Electrical Recording and Local Thermal Control in Sleep Spindle Oscillation Studies. *Procedia Engineering, 168*, pp.109-112. https://doi.org/10.1016/j.proeng.2016.11.159

1.4.2. **Conference presentations**

1.4.2.1. **First-author presentations**

[C1] Kocsis K, Csernai M, Horváth Á, Fekete Z, Barthó P (2016): Body temperature modulates sleep spindle frequency. Poster, IBRO Workshop, Budapest, Hungary.

[C2] Kocsis K, Csernai M, Horváth Á, Fekete Z, Barthó P (2016): Body temperature modulates sleep spindle frequency. Poster, HuNDoC, Budapest, Hungary.

[C3] Kocsis K (2015): Effects of body temperature on the occurrence and parameters of sleep spindles. Talk and conference paper*, PhD Proceedings, Annual Issues of the Doctoral School, Faculty of Information technology and Bionics, 10*: pp. 65-68.

[C4] Kocsis K, Csernai M, Barthó P (2015): Spindle frequency is modulated by body temperature. Poster, 15th Biannual Meeting of the Hungarian Neuroscience Society, Budapest, Hungary.

1.4.2.2. **Co-author presentations**

[C5] Csernai M, Kocsis K, Burka D, Borbély S. Fekete Z, Balogh V, Káli S, Emri Z, Barthó P (2018): Sleep spindle frequency is modulated by temperature in vivo and in silico. Poster, FENS Forum, Berlin, Germany.

[C6] Csernai M, Kocsis K, Burka D, Borbély S, Fekete Z, Balogh V, Káli Sz, Emri Z, Barthó P (2017): Temperature modulates sleep spindle frequency in vivo and in silico. Poster, Annual Meeting of the Society for Neuroscience (Neuroscience 2017), Washington DC, U.S.

[C7] Fekete Z, Kocsis K, Horváth Á, Barthó P (2016): A novel neural probe for simultaneous electrical recording and local thermal measurements in sleep spindle oscillation studies. Poster, Biosensors 2016, Göteborg, Sweden.

PART 2 Study of aversive cue discrimination in the thalamus

2.1. Motivation and aims of the study

There are many burning questions regarding how affective interpretation of environmental stimuli is established. One of them is how precortical neural processing channels aversive signals in order to achieve rapid discrimination under threat, ultimately promoting survival. Subcortical evaluation of external cues often precedes the extensive and fine processing of their physical properties, helping to elaborate adaptive behavior.

Auditory fear conditioning is a Pavlovian (classical) behavioral paradigm used to establish robust aversive learning. It drives lab rodents to associate a previously neutral cue (conditioned stimulus, CS; e.g., a sine wave) to an aversive (unconditioned) stimulus (US; e.g., electric foot shock). According to a vast literature, this multisensory integration and memory formation can be tracked by synaptic changes in the lateral amygdala (LA) (Nabavi *et al.*, 2014). Consequently, the future presentation of the CS reliably elicits defensive responses, such as freezing or escaping. Nevertheless, the question arises about the nature of this plasticity regarding the inputs arriving to amygdala territory.

The monosynaptic, subcortical connections between the thalamus and the amygdala, two evolutionarily conserved brain structures, have been proposed as key routes in fast (<20 ms) cue association. Studies in the 80s revealed a shortcut to the amygdala, formed by cell populations in the posterior region of the medial geniculate nucleus (MGN), the primary thalamic station of auditory processing. These lateral thalamic regions, including the posterior intralaminar (PIL) and suprageniculate (SG) thalamic nuclei as well as the medial and dorsal part of the MGN (MGM and MGD, respectively) form monosynaptic connections with the LA (LeDoux *et al.*, 1990). In particular, the MGM is traditionally accepted as the major source of the auditory CS (LeDoux *et al.*, 1984).

The source of US information in the LA, which can temporally match the CS signal is rather debated despite the fact that the possibility of an associative auditory-nociceptive CS-US convergence and response facilitation in the lateral thalamus has been shown (see (Weinberger, 2011)). The diversity of lateral thalamic nuclei, an ever-changing anatomical delineation and inconsistent terminology across species and studies as well as the focus on sole and purely sensory modalities in the thalamus derailed the tendencies that highlighted the integrative and operative thalamic role in learned threat-evoked behaviors.

Based on the above-noted, the need arises for the functional dissection of the thalamic cohort that projects to the amygdala setting the basis for robust and preconscious affective processing in threatening experiences. In this part of my studies, I was driven to provide new insight into the lateral thalamic role in aversive learning.

- I studied the responsivity of cells in the non-canonical auditory thalamic region to neutral as well as to single and associated aversive (threat-derived) cues in urethane-anesthetized and freely behaving mice (**Aim IIa**);
- I intended to elucidate whether lateral thalamic neurons can directly convey single and associated aversive cues to the lateral region of the amygdala (**Aim IIb**);
- I investigated the possible collicular underpinnings for the time-course of activation and cue-responsivity of the direct lateral thalamo-amygdala route (**Aim IIc**).

2.2. Experimental approaches

Our group cell-specifically classified the LA-projecting thalamic neurons with retrograde labelling technique (cholera toxin B subunit injection): they are principally located in the vicinity of the primary auditory thalamus (MGN), in the PIL and the SG, and the majority (~94%) of them express calretinin (CR) (Barsy & Kocsis *et al.*, 2020). I collectively refer to them as CR+ lateral thalamic (CR+LT) ensemble, and I hereby probed calretinin as a marker to functionally dissect the direct lateral thalamo-amygdala route.

Acute extracellular neural data acquisition was performed in urethane-anesthetized, male and female mice (>3 months old) in order to study whether the direct lateral thalamo-amygdala route can encode and possibly integrate neutral and innately aversive sensory cues. Thalamic (n=16 mice) activity was monitored with Buzsáki32 silicon probes, amygdala (n=25 mice) recordings were done with Buzsáki32, 64, or 256 probes (NeuroNexus Technologies). Wideband neural data (0.1-7500 Hz) were amplified (gain: 192 or 400 V/V), and digitized at 20 kHz (RHD2132 or RHD2164, Intan Technologies or Amplipex). Orthodromic and antidromic optogenetic activations consisted of 473 nm blue light pulses (Laserglow Technologies) and served the identification of virally transduced neurons. The stimulation protocols were executed with custom-written MATLAB codes. All analog trigger pulses were delivered to the evaluation board for synchronization purposes.

IIa-b. Auditory and foot shock-evoked responses were tested in the thalamus and the amygdala subnuclei of Cre-dependent virus (AAV-DIO-ChR2-eYFP or AAV-DIO-NpHR3.0-eYFP) injected Calb2(CR)-Cre mice (**Figures 2.3.1.1./a** and **2.3.2./a, c**). In the case of acoustic stimulations, the animal's head was fixed with a head plate in the stereotaxic frame. The auditory signal was a 7.5 kHz pure tone (1 s or 30 s, 75-85 dB). Foot shock was achieved by bipolar electric stimulation (50/100 ms or 1 s, 1 mA) of a paw, which resulted in pain reflex. The lasers and the speaker as well as the current generator (Medicor or BioStim Bipolar Stimulus Isolator BSE-4x, Supertech Instruments or STG4008-1.6mA, Multi Channel Systems) were triggered by a National Instruments acquisition board (NI USB-6353).

IIa. To clarify whether CR+LT cells show experience-dependent activity throughout aversive learning, Calb2-Cre mice (n=33) were unilaterally injected with AAV-DIO-ChR2-eYFP into the amygdala or the thalamus (**Figure 2.3.1.2./a**). 4-6 weeks after AAV injection, four custom fabricated tungsten tetrodes (d=12.5 µm, California Fine Wire) were chronically implanted into the lateral thalamus (LT) and also into the amygdala in additional cases. They were inserted along with a multimode optic fiber (105 µm core diameter, Thorlabs), all tunneled in a polyimide tube (203 µm internal diameter, Neuralynx). The tetrode wires were attached to an electrode interface board (EIB-16 and EIB-36 Narrow, Neuralynx). During the behavioral protocol, the EIB was connected to the Intan RHD2000 recording system via an RHD2132 preamplifier. I monitored unit activity during aversive conditioning and cued memory retrieval, besides ortho- and antidromic optogenetic identifications (473 nm). Delivery of the 1 s foot shocks (Ionflow Bipolar or BioStim Bipolar Stimulus Isolator BSE-4x, Supertech Instruments) and auditory stimulations was triggered by analog signals (NI USB-6343) and registered in parallel with the neural data. Auditory stimuli (75 dB) were composed of 30 s (additionally also 3 and 10 s) long 7.5 kHz sine waves (CS+) and Gaussian white noises (CS-). Aversive mouse behavior was manually annotated and quantified by the time percentage of freezing with the H77 recorder software (courtesy of Prof. Dr. József Haller), or in the additional cases, with a custom-written locomotion analysis pipeline in Bonsai (Lopes *et al.*, 2015).

IIb. To test the functional impact of the CR+LT innervation on the lateral amygdala region including the LA and the amygdalostriatal transition area (Astr), CR+LT neurons were transduced with halorhodopsin (NpHR3.0) expressing AAV, and *in vivo* extracellular recordings (n=11) were performed in the amygdala (**Figure 2.3.2./c**). I investigated the contribution of the direct CR+LT projections to sensory activations in the amygdala by silencing CR+ axons (532 nm) during cue delivery.

Broadband electrophysiological recordings were filtered (>500 Hz). Spike detection and automatic clustering were performed with SpikeDetekt and KlustaKwik, respectively (Rossant *et al.*, 2016). Cell grouping was refined manually with KlustaViewa. I carried out all further data analysis with custom-built MATLAB codes. In the case of amygdala neurons, putative principal (PN) and interneurons (IN) were distinguished based on the bimodal distribution of trough-to-peak and half-amplitude spike width of their mean action potential waveform.

Light-evoked spiking within 10 ms ($z>3.3$) was considered reliable to indicate direct and monosynaptic somatic or axonal activation. Significant sensory evoked responses were defined by setting a Poisson-distribution based confidence interval ($p<0.05$) for a 1 s long baseline before stimulations, and a signal-to-noise ratio ($\mu/\sigma>0.5$) criterion in the case of short-latency (<50 ms) responses. Response latencies (in 2.5/5 ms bins) were estimated from the first bin value larger than 3 in the z-scored peristimulus time histogram (PSTH). Enhancement in multimodal responses was defined as the increase compared to the sum of average tone and shock-evoked firing rates.

IIc. I identified the distribution of collicular inputs in the CR+LT region with anterograde viral tracing. To test both glutamatergic (excitatory, vGluT2+) and GABAergic (inhibitory, vGAT+) midbrain innervation of the CR+LT, I injected Cre-dependent enhanced Yellow Fluorescent Protein (eYFP) expressing AAV into the inferior (IC) and superior (SC) colliculus of vGluT2-Cre (n=3-3, **Figure 2.3.3./a-b** and **j-k**, respectively) and vGAT-Cre mice (n=2-2, **Figure 2.3.3./q-r** and **t-u**, respectively). In order to amplify virally expressed fluorophore signals (eYFP), fluorescent immunohistochemistry was performed. Synaptic contacts formed by the collicular inputs on CR+LT neurons (n=3-3) were visualized with electron microscopy.

2.3. New scientific contributions

2.3.1. **Thesis IIa**

I showed with extracellular electrophysiological recordings in urethane-anesthetized and freely behaving mice that lateral thalamic calretinin-positive (CR+LT) neurons process both neutral auditory and aversive (nociceptive or threat-related auditory) cues. They exhibit multisensory and associative enhancement on a single neuronal level.

Related journal publication: [J4]

I participated in the conception, design and methodological foundation of the electrophysiological and behavioral experiments. I carried out surgeries, viral injections and implantations, I carried out the behavioral tests. I performed the acquisition, analysis and interpretation of the acute and chronic electrophysiological data. I took part in the drafting and revision of the related section of the manuscript.

Related conference presentations: [C10]-[C16], [C21]

Foot shock (FS) and foot shock-paired tone stimuli activated more LT cells than tone alone. Short-latency (<50 ms) nociceptive cue responses were primarily characteristic to the CR+ PIL populations, which is in concordance with the aversive activition previously shown in this region (Bordi & LeDoux, 1994; Lipshetz *et al.*, 2018). Overall, a higher proportion of CR+ PIL neurons were receptive to foot shock and associative stimuli than CR- PIL cells. However, SG units showed late aversive activation (50-500 ms) in a higher proportion, with no significant difference between the CR+ and the non-tagged cohort (**Figure 2.3.1.1./b-d**).

Aversive uni- and multimodal response latencies of the CR+ PIL were shorter than the ones evoked by single tone presentations. Moreover, paired signals drove the strongest short-latency activation (~17 ms on average, **Figure 2.3.1.1./e-f**) in this population. Their phasic activations underwent multisensory enhancement even in the absence (83%) of unimodal acoustic responses (**Figure 2.3.1.1./g**), suggesting that auditory stimulation may evoke subthreshold activation. Yet it can potentiate nociceptive signaling in these cells.

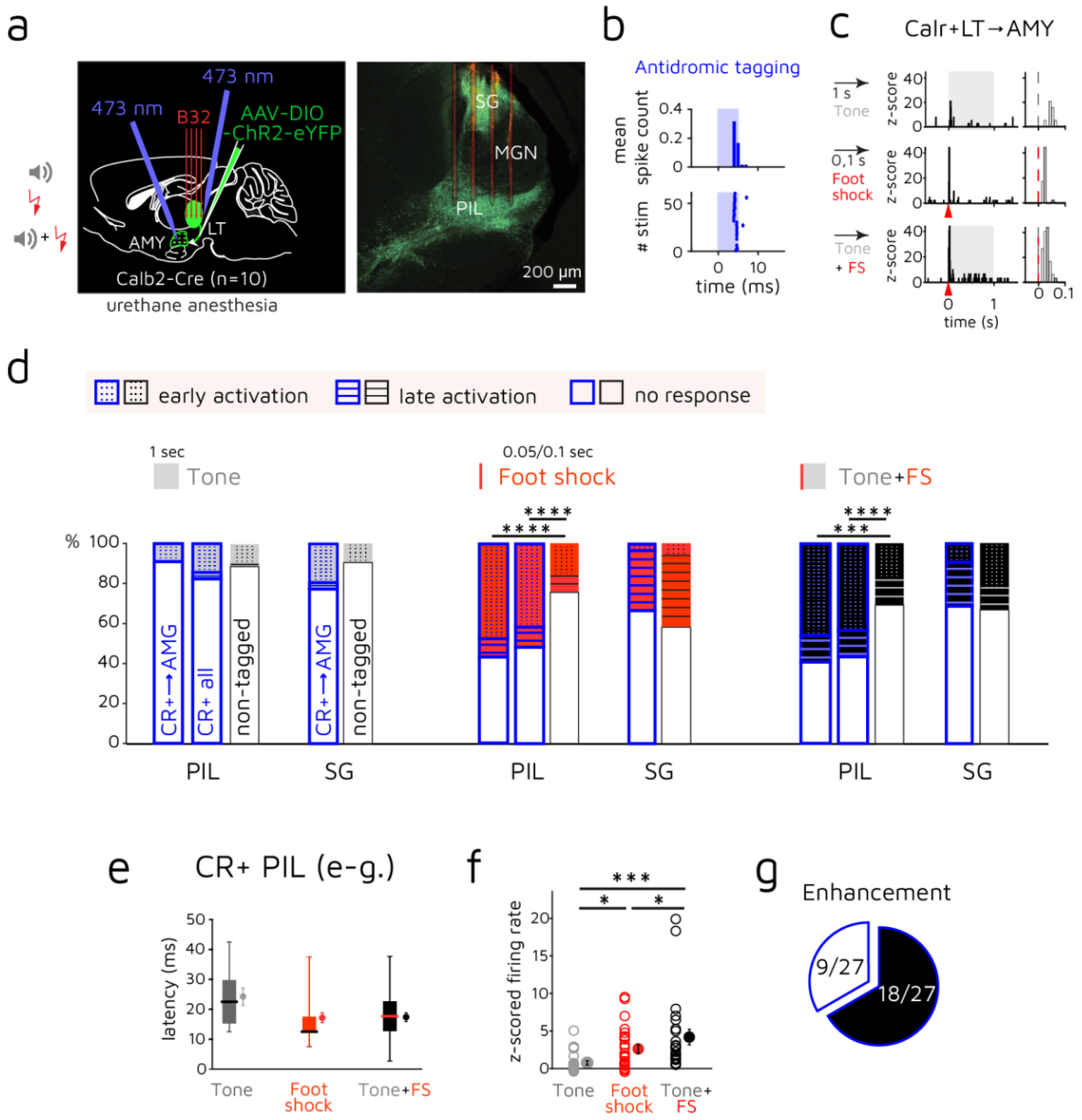

Figure 2.3.1.1. Selective and fast aversive sensory signaling by the CR+LT.

a/ Left: scheme for acute *in vivo* electrophysiological recordings from LT cells (n=10 mice) with delivery of tone, foot shock and joint tone+foot shock signals as well as of ortho- and antidromic optogenetic stimuli for identification purposes. Right: a coronal section with AAV-DIO-ChR2-eYFP-transduced CR+ cells (green) and the trace of the four-shank Buzsáki32 probe (B32, red). **b/** Antidromic optogenetic tagging (blue shade) of a CR+LT→AMY cell. Bin size of the PSTH is 1 ms. **c/** A CR+LT→AMY unit showing short-latency tone (gray shade), foot shock (FS; red arrowhead) and enhanced paired tone+foot shock activation. Right: zoom-in of the traces on the left. Bin size is 10 ms. **d/** Graphs showing the proportions of short-latency (<50 ms, dotted area) and long-latency (50-500 ms, striped area) tone- (gray), foot shock- (FS; red) and paired tone+foot shock-evoked (black) responses within the CR+LT→AMY and the total CR+LT (blue framed boxes) as well as within the non-tagged LT cell populations (black framed boxes), all divided into PIL and SG units. Note that the CR+ PIL unit responses are mostly short-latency (<50 ms). *χ^2 test*. **e/** Boxplots showing the estimated latencies of early sensory activations in the CR+ PIL cells within a 50 ms poststimulus time window. Filled circles represent the mean ± SEM. **f/** Average z-scores of short-latency (<50 ms) unit firing rates upon sensory stimulations in the case of CR+ PIL neurons with short-latency associated responses (N = 27 cells). Mean ± SEM. *Friedman's ANOVA with Wilcoxon signed-rank test (two-sided)*. **g/** Proportion of multisensory enhancement (augmented tone + foot shock signaling) among the CR+ PIL cells in **f**.

Published in (Barsy & Kocsis et al., 2020) Figure 2., supplemented with SG/MGN recordings.

CR+LT in freely behaving mice also showed short-latency (<50 ms) auditory response modulation in parallel with the formation of an aversive memory (**Figure 2.3.1.2./b-c**). Threat learning recruited CR+LT→AMY neurons to respond to the aversive CS+. This indicates that the CR+LT→AMY pathway can transfer associated signals in behaving animals, as its sensory activity can change with an aversive association.

I have provided evidence that the association of tone and foot shock can take place at the level of the thalamus, prior to the amygdala, and this feature can be captured by studying the CR+ PIL population. This does not simply manifest in the recruitment of active neurons, but also on a single cellular level. These associated activations can then be conveyed to the amygdala, which supports fast defensive responses. These observations further challenge the widely accepted concept that the LA is the first site of CS-US association. My findings have been reviewed by (Gründemann, 2021), raising awareness to a distributed subcortical neuronal network function in defensive behavior.

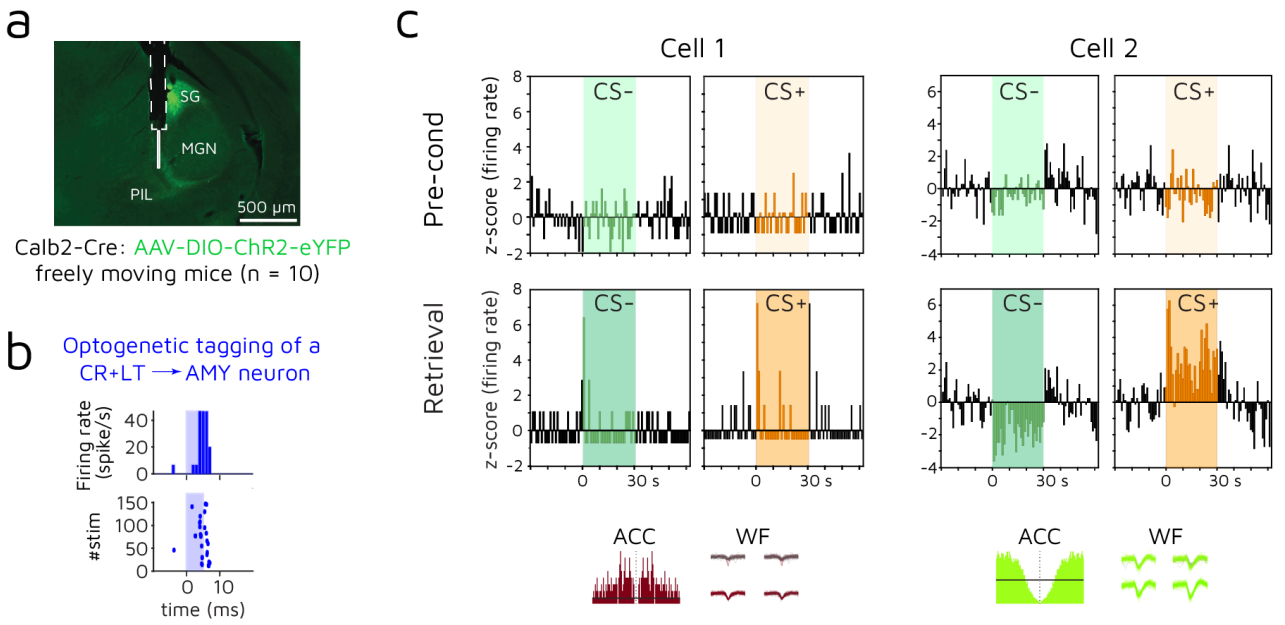

Figure 2.3.1.2. Discriminative auditory aversive learning induces changes in the activity pattern of CR+LT cells.

a/ A coronal section showing retrogradely labeled CR+LT→AMY cells (green) and the location of the ensemble of optic fiber and tetrodes (white scheme). ***b/*** Optogenetic tagging (blue) of a CR+PIL→AMY cell, also shown as Cell 1 in **c**. Bin size is 1 ms. ***c/*** Auditory evoked activities (CS-: green, CS+ orange shaded areas) of two CR+LT→AMY cells before conditioning (Pre-Cond) and during cued fear retrieval (Retr). Note the elevated onset (cell 1 and cell 2) and offset (cell 1) responses to CS+ upon threat learning. Autocorrelograms (ACC; left) and waveforms (WF; right) of the units from the respective tetrode channels are shown below. Horizontal line on the ACC indicates the asymptote line, vertical dotted line shows the center. Bin size is 1 s.

Published in (Barsy & Kocsis et al., 2020) Figure 7./h,j,k and Supplementary Figure 8./c-e.

2.3.2. **Thesis IIb**

I found in urethane-anesthetized mice with extracellular electrophysiological recordings that calretinin-positive lateral thalamic (CR+LT) neurons can directly convey aversive uni- and multimodal cues to the lateral region of the amygdala where their signaling recruits narrow-spiking neurons.

Related journal publication: [J4]

I participated in the conception, design and the methodological foundation of the electrophysiological experiments. I carried out surgeries and viral injections, as well as the acquisition, analysis and interpretation of the acute electrophysiological data. I took part in the drafting and revision of the related section of the manuscript.

Related conference presentations: [C8], [C10]-[C14], [C20], [C21], [C27], [C28]

I confirmed that calretinin-positive (CR+) neurons in the lateral thalamus fulfill the prerequisites for the function of direct thalamo-amygdala pathways in auditory threat conditioning: besides auditory cues, they can directly convey short-latency nociceptive and integrated signals to the subcortical region of aversive learning, the lateral region of the amygdala.

Both in the case of CR+LT→AMY optogenetic activation and foot shock stimuli, spatiotemporal maps of the evoked activation placed the earliest amygdala activation in the lateral amygdala (LA) and the adjacent amygdalostriatal transition area (AStr) (**Figure 2.3.2./b**). This confirms that these areas together provide the sensory interface for the lateral thalamus (LeDoux *et al.*, 1990) in threat learning.

Nociceptive single and associated cue-evoked responses were the shortest latency (~20 ms) and strongest activities in the recorded amygdala (LA/AStr) populations, similarly to CR+LT neurons. The time course of aversive activation in the CR+ PIL and the amygdala (2-3 ms difference in latency on average) also suggests that aversive short-latency amygdala activation can be directly derived from the CR+LT.

Aversive cue responsivity was particularly abundant amongst narrow-spiking neurons. Moreover, direct optogenetic CR+LT-mediated modulations, be they excitatory or inhibitory, affected them to a larger extent (**Figure 2.3.2./d-e**). In addition to the suppressed responses, many neurons enhanced their sensory evoked activation or only showed responses during CR+LT→AMY optogenetic silencing, implying a thalamus-driven inhibitory/disinhibitory mechanism in the lateral region of the amygdala.

Thus, thalamic inputs, fulfilling an imminent need to prioritize threatening cues, may directly drive population selection by targeting amygdala interneurons: (1) establishing a window of phasic elevation in firing rates (Pouille & Scanziani, 2001), as well as potential synchronization, (2) suppressing the cohort activities which do not serve saliency detection, and (3) regulating plasticity along the somatodendritic axis of principal neurons.

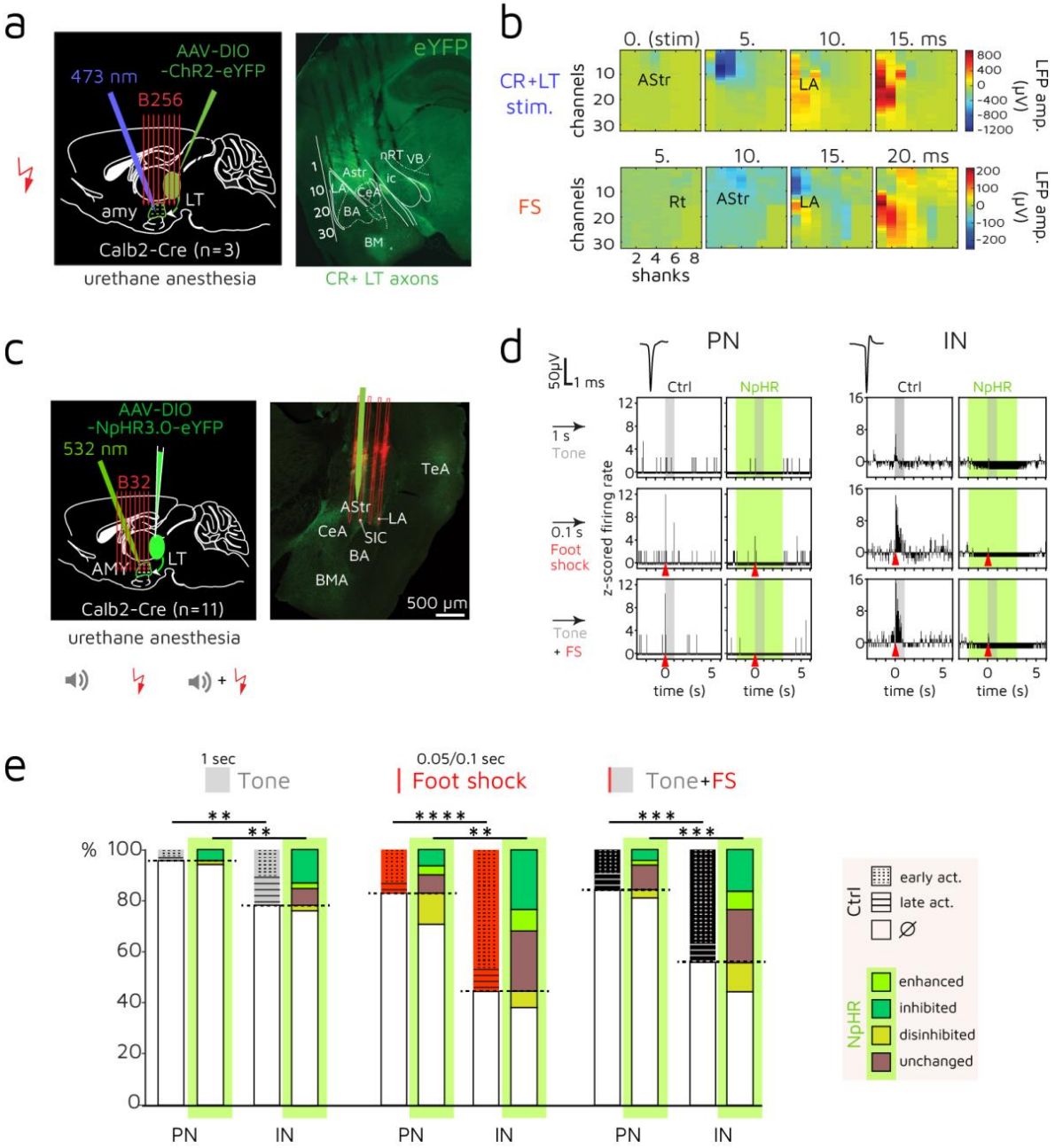

Figure 2.3.2. CR+LT neurons directly control the sensory activation of amygdala cells.

a/ Scheme (left) for acute *in vivo* electrophysiological recordings from the amygdala with foot shock stimulation and optogenetic excitation of AAV-DIO-ChR2-eYFP-transduced CR+LT→AMY inputs. A coronal section (right) showing the incoming transduced CR+LT fibers (eYFP, green) and the electrode insertion tracks in the amygdala. Scheme for the amygdala nuclei is overlayed. ***b/*** Representative snapshots (in ms) of the mean evoked responses in broadband activity across the 256 probe channels (32 channels on 8 shanks) covering the amygdala. Optogenetic and shock-evoked responses are shown in two rows, shifted with 5 ms for comparative purposes. ***c/*** Scheme (left) for acute *in vivo* electrophysiological recordings from the amygdala with sensory stimulations and optogenetic inhibition of AAV-DIO-NpHR-eYFP-labeled CR+LT→AMY terminals. A representative coronal section (right) showing the insertion tracks of the optic fiber (green) and a four-shank DiI-stained Buzsáki32 probe (red) placed in the amygdala. ***d/*** Sensory responses of a putative principal (PN) and interneuron (IN) in control condition and during optogenetic inhibition (green) of CR+LT inputs. Gray shadings represent tone delivery, red arrowheads mark the delivery of foot shock (FS) stimuli. Bin size is 50 ms. Mean spike waveforms are shown above the PSTHs. ***e/*** Population data for tone-, foot shock- (FS) and tone+FS-evoked activities of amygdala neurons divided into putative principal cells (PN) and interneurons (IN). Evoked responses in control conditions and response modulations during NpHR-mediated CR+LT→AMY axonal inhibition (graphs with green frame) are shown. χ^2 *test*.

Panels c-d published in (Barsy & Kocsis et al., 2020) Figure 5./a,b,d.

2.3.3. **Thesis IIc**

I confirmed with anterograde viral tracing in mice that the calretinin-positive lateral thalamic (CR+LT) population relies on a non-primary and multimodal midbrain innervation from the inferior (IC) and superior (SC) colliculi. The CR+LT region is exclusively targeted by the superior colliculus.

Related journal publication: [J4]

I participated in the conception and design of the anatomical investigation. I carried out the surgeries and viral injections, I participated in the anatomical processing and the interpretation of the results. I took part in the drafting and revision of the related section of the manuscript.

Related conference presentations: [C9]-[C13], [C21]

The above-stated theses added several lines of evidence for the multisensory aspect of the CR+LT function, and highlighted the potential importance of collothalamic processing, which can reach beyond parallel sensory transmissions, and perform cue integration / discrimination before any amygdala computation. The functional anatomical basis for this is established by a midbrain innervation with non-primary and multimodal character, also distinct from the one in the adjacent primary auditory thalamus (MGN). I showed that CR+LT cells are targeted by sparse and small (diameter(d)<1 µm) excitatory (vGluT2+) terminals from the ipsilateral inferior colliculus (IC) in contrast to the MGN with large (d~3-5 µm) IC boutons (**Figure 2.3.3./c-h**); the superior colliculus (SC) exclusively targets the CR+ PIL/SG region (**Figure 2.3.3./l-m**). Asymmetrical (excitatory) synaptic contacts between IC / SC inputs and the CR+LT were confirmed with electron microscopy (**Figure 2.3.3./i**, and **n-p**, respectively). vGAT+ (inhibitory) IC and SC neurons had a similar projection pattern to excitatory ones (**Figure 2.3.3./s**, and **v**, respectively).

Such collicular innervation can promote CR+LT neurons to rapidly integrate cues upstream to the amygdala and the neocortex, potentially both from neutral sensory and ethologically relevant integrated information, which could provide a subcortical bypass from elaborated primary sensory processes under threat. CR+LT-projecting brainstem regions have the potential to transfer short-latency auditory (IC), visual (SC), nociceptive (SC) (Stein & Dixon, 1978) as well as multimodal (SC/IC) cues (Hayashi *et al.*, 1984; Linke *et al.*, 1999). Moreover, as the mouse thalamus typically lacks local inhibitory control, the interplay between excitatory and inhibitory midbrain afferents can further enhance the computational capacities of the thalamic population, in addition to reticular inhibition, increasing the signal-to-noise ratio of aversive processing in the CR+LT (**Figure 2.3.3./w**).

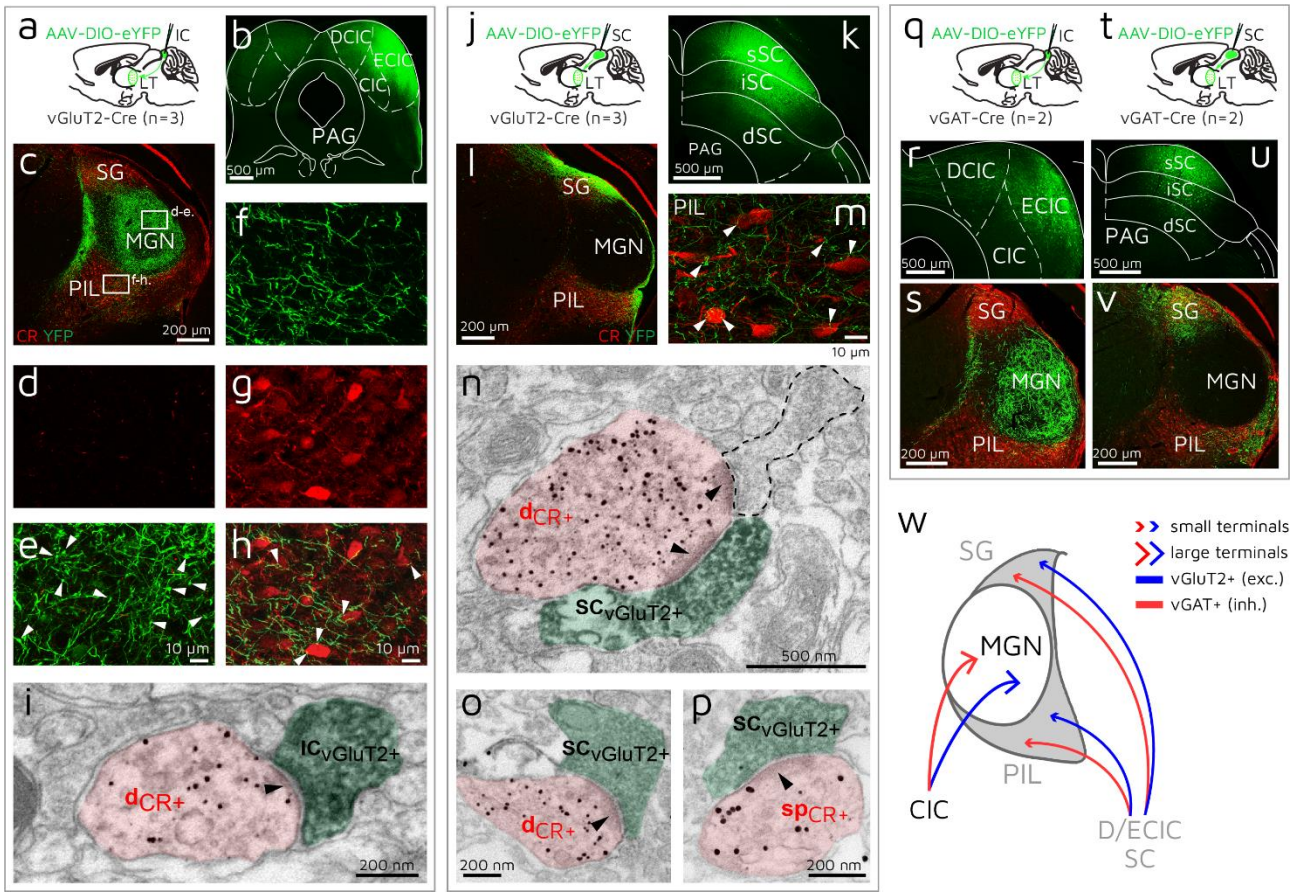

Figure 2.3.3. Collicular innervation of the CR+LT region is non-primary and multimodal.

a/ Scheme for AAV-DIO-eYFP injections into the inferior colliculus (IC) of vGluT2-Cre mice. ***b/*** Injection site in the IC. ***c/*** vGluT2+ IC inputs (eYFP, green) in the LT, which is co-stained for CR (red). White framed areas are enlarged in **d-e** and **f-h**. ***d-e/*** z-stack confocal images (7 µm total depth) from the MGN (CR- area in **d**) showing large-sized IC axon terminals (white arrowheads in **e**). ***f-h/*** z-stack confocal image (7 µm total depth) from the PIL (red CR-staining in **g**) illustrating small-sized IC axon terminals (**f**; white arrowheads in **h**) in the vicinity of CR+ PIL cells. ***i/*** Electron micrograph showing an immunogold-labeled CR+ dendrite in the PIL (dCR+; covered by small black particles; shaded with pink) receiving an asymmetrical synaptic contact (black arrowhead) formed by a DAB-labeled (diffuse black precipitate) vGluT2+ IC axon terminal (ICvGluT2+; shaded with green). ***j/*** Scheme for AAV-DIO-eYFP injections into the superior colliculus (SC) of vGluT2-Cre mice. ***k/*** Injection site in the SC. ***l/*** vGluT2+ SC inputs (eYFP, green) in the LT, which is co-stained for CR (red). ***m/*** z-stack confocal image (7 µm total depth) with vGluT2+ SC axon terminals (white arrowheads) in close proximity to CR+ PIL neurons (red). ***n-p/*** Electron micrographs showing immunogold-labeled CR+ dendrites (dCR+ in **n-o**) and a spine (spCR+; **p**) in the PIL receiving asymmetrical synaptic contacts (black arrowheads) from DAB-labeled, vGluT2+ SC axon terminals (SCvGluT2+). A non-stained axon terminal with dashed outline (in **n**) also gives synaptic input onto the CR+ dendrite. ***q/*** Scheme for AAV-DIO-eYFP injections into the IC of vGAT-Cre mice. ***r/*** Injection site in the IC. ***s/*** vGAT+ IC inputs in the LT, which is co-stained for CR. ***t/*** Scheme for AAV-DIO-eYFP injections into the SC of vGAT-Cre mice. ***u/*** Injection site in the SC. ***v/*** vGAT+ SC inputs (YFP, green) in the LT, which is co-stained for CR (red). ***w/*** Schematic drawing for the collicular inputs of CR+LT territories (PIL/SG) in contrast to those of the primary auditory nucleus (MGN).

*Panels **a-p** published in (Barsy & Kocsis et al., 2020) Figure 3./h-w.*

2.3.4. **Outlook: future directions and potential for the study**

A fruitful follow-up could be the exploration of how CR+LT inputs orchestrate the amygdala network to provide a robust processing of ethologically relevant signals by recruiting and/or synchronizing cell ensembles. The CR+LT strongly shapes the activity of interneurons that are able to determine the functional network configuration: they select the principal cells involved in coding and they are linked to oscillation generation.

The LT has also got a unique connection to neuroendocrine networks. (Barsy & Kocsis *et al.*, 2020) showed that the CR+LT projects to the ventromedial hypothalamus. (Cservenak *et al.*, 2017) described a pathway from the PIL to the paraventricular hypothalamic nucleus in mice, which can trigger oxytocin release in lactating mothers by processing the pups' somatosensory cues. Relatedly, (Tasaka *et al.*, 2020) showed that the temporal associative cortex, a CR+LT target area (Barsy & Kocsis *et al.*, 2020), plays a key role in discriminating ultrasonic pup vocalizations by mothers. These studies imply that behaviorally relevant cue processing of the CR+LT may potentially drive hormonal changes that can further enhance stimulus selection in its target regions. Moreover, as 'belt' LT regions integrate visual and reward cues (Komura *et al.*, 2005), the CR+LT population could also contribute to the extraction of affective content from movements (e.g., gestures) related to vocal behavior (Bartlett, 2013).

Overall, I point towards investigations with a focus on the CR+LT role in non-conscious affective cue processing. This population can be a potential target of modulation or molecular genetic characterization in affective disorders which involve enhanced or attenuated affective cue processing. Therapeutic strategies aimed at treating implicit associative processes in affective disorders might consider altering the cue integration of this neuronal group.

2.4. Relevant publications

2.4.1. **Peer-reviewed articles**

Publication supporting the theses

[J4] Barsy B*, Kocsis K*, Magyar A, Babiczky Á, Szabó M, Veres MJ, Hillier D, Ulbert I, Yizhar O, Mátyás F (2020): Associative and plastic thalamic signaling to the lateral amygdala controls fear behavior. *Nature Neuroscience*, *23(5):* pp. 625-637. https://doi.org/10.1038/s41593-020-0620-z

*shared first authorship

Other relevant publication

[J5] Mátyás F*, Komlósi G*, Babiczky Á, Kocsis K, Barthó P, Barsy B, Dávid Cs, Kanti V, Porrero C, Magyar A, Szűcs I, Clasca F, Acsády L (2018): A highly collaterized thalamic cell type with arousal predicting activity serves as a key hub for graded state transitions in the forebrain. *Nature Neuroscience, 21(11):* pp. 1551-1562. https://doi.org/10.1038/s41593-018-0251-9

2.4.2. **Conference presentations**

2.4.2.1. **First-author presentations**

[C8] Kocsis K (2020): The role of thalamic inputs in amygdala oscillation generation. Talk, 'Subcortical neural processing of saliency' online minisymposium, University of Veterinary Medicine.

[C9] Kocsis K, Jártó F, Zsoldos R, Zsebők S, Mátyás F (2020): Ultrasonic adult distress vocalizations and their subcortical neural processing in laboratory mice. Speed talk, 2nd African Bioacoustics Community Conference.

[C10] Kocsis K, Magyar A, Barsy B, Babiczky Á, Mátyás F (2019): Cell-type-specific interrogation of the mouse thalamus in aversive cue processing. Poster, Annual Meeting of the Hungarian Neuroscience Society, Debrecen, Hungary.

[C11] Kocsis K, Magyar A, Barsy B, Babiczky Á, Jártó F, Váncsodi M, Berényi A, Mátyás F (2019): The role of thalamic cells in amygdala-related processes. Poster, FENS-Hertie Winter School 2018 – Neural control of innate and instinctive behaviour, Obergurgl, Austria.

[C12] Kocsis K, Magyar A, Barsy B, Babiczky Á, Kanti V, Truka L, Szabó M, Jártó F, Váncsodi M, Berényi A, Mátyás F (2018): Nucleus-specific interrogation of the mouse thalamus in aversive cue-processing. Poster, Annual meeting of the Society for Neuroscience (Neuroscience 2018), San Diego, CA, U.S.

[C13] Kocsis K, Magyar A, Barsy B, Babiczky Á, Jártó F, Váncsodi M, Berényi A, Mátyás F (2018) Calretinin-positive thalamic neurons convey distinct information in aversive learning. Poster, FENS Forum, Berlin, Germany.

[C14] Kocsis K, Barsy B, Magyar A, Babiczky Á, Kanti V, Horváth M, Varga K, Földes TA, Mátyás F (2017): Pathway-specific thalamic modulation of amygdalar circuits. Poster, Annual meeting of the Society for Neuroscience (Neuroscience 2017), Washington DC, U.S.

[C15] Kocsis K*, Magyar A*, Barsy B, Kanti V, Babiczky Á, Varga K, Földes TA, Mátyás F (2017): Functional investigation of thalamoamygdalar circuits in freely behaving mice. Poster, FENS Regional Meeting, Pécs, Hungary.

[C16] Kocsis K*, Magyar A*, Barsy B, Kanti V, Babiczky Á, Varga K, Földes TA, Mátyás F (2017): Functional investigation of thalamoamygdalar circuits in freely behaving mice. Poster, HuNDoC, Pécs, Hungary.

[C17] Kocsis K, Barsy B, Babiczky Á, Magyar A, Kanti V, Ulbert I, Mátyás F (2016): Role of the thalamoamygdalar circuitry in fear behavior. Poster, From Bionics to Medicine – 3rd European PhD Conference, Budapest, Hungary.

[C18] Kocsis K, Barsy B, Ulbert I, Mátyás F (2016): Cell-type specific investigation of the thalamo-amygdala network in associative learning. Poster, FENS Forum, Copenhagen, Denmark.

[C19] Kocsis K (2016): Functional investigation of non-canonical pathways originating from the auditory thalamus. Talk and conference paper, *PhD Proceedings, Annual Issues of the Doctoral School, Faculty of Information technology and Bionics, 11*: pp. 59-6.

2.4.2.2. **Co-author presentations**

[C20] Jártó F, Váncsodi M, Magyar A, Berényi A, Mátyás F, Kocsis K (2020): Closed-loop optogenetic manipulation of amygdalar network activity based on local gamma band oscillations. Poster, IBRO Workshop, Szeged, Hungary.

[C21] Kocsis K*, Barsy B*, Babiczky Á, Szabó M, Magyar A, Váncsodi M, Jártó F, Berczik J, Fehér A, Hillier D, Yizhar O, Berényi A, Mátyás F (2019): Thalamic control over amygdala function. Talk, Gordon Research Conference, 2019, Easton, MA, U.S.

[C22] Jártó F, Kocsis K, Barsy B, Váncsodi M, Magyar A, Szabó M, Kanti V, Mátyás F (2019): Automated monitoring and closed loop modulation of affective behavior-related parameters in mice. Poster, FENS-SfN Summer School – Brain reading and writing: new perspectives of neurotechnology. Bertinoro, Italy.

[C23] Nagy GA, Magyar D, Kocsis K, Veres JM, Pardo-Bellver C, Reéb Zs, Földi P, Mátyás F and Hájos N (2019): Parallel processing of noxious stimuli in the basolateral amygdala circuits. Talk, KOKI Napok 2019.

[C24] Jártó F, Kocsis K, Barsy B, Magyar A, Szabó M, Kanti V, Mátyás F (2019): A modular, automated closed loop stimulation system for acquisition and evaluation of behavioral experiments. Poster, Annual Meeting of the Hungarian Neuroscience Society, Debrecen, Hungary.

[C25] Szabó M, Barsy B, Kocsis K, Jártó F, Magyar A, Mátyás F (2019): Essential role of the lateral thalamoamygdalar pathway in fear learning. Poster, Annual Meeting of the Hungarian Neuroscience Society, Debrecen, Hungary.

[C26] Szabó M, Barsy B, Kocsis K, Jártó F, Magyar A, Mátyás F (2019): Essential role of the lateral thalamoamygdalar pathway in fear learning. Poster, HuNDoC, Debrecen, Hungary.

[C27] Váncsodi M, Kocsis K, Babiczky Á, Szabó M, Berényi A, Mátyás F (2019): Electrophysiological characterization of the cell-type specific thalamic effects on the amygdalar microcircuit, Poster, Annual Meeting of the Hungarian Neuroscience Society, Debrecen, Hungary.

[C28] Váncsodi M, Kocsis K, Babiczky Á, Szabó M, Berényi A, Mátyás F (2019): Electrophysiological characterization of the cell-type specific thalamic effects on the amygdalar microcircuit, Poster, HuNDoC, Debrecen, Hungary.

[C29] Babiczky Á, Kanti V, Barsy B, Magyar A, Horváth M, Szabó M, Truka L, Kocsis K, Hillier D, Yizhar O, Mátyás F (2018): Nucleus-specific connectivity of the fear-related auditory thalamus. Poster, FENS Forum, Berlin, Germany.

[C30] Barsy B*, Kocsis K*, Babiczky A, Magyar A, Szabó M, Kanti V, Horváth M, Váncsodi M, Jártó F, Pinke D, Hillier D, Yizhar O, Acsády L, Berényi A, Mátyás F (2018): Szenzoros információk által kiváltott viselkedés-válaszreakciók komplex mechanizmusa. Poster, Magyar Tudomány Ünnepe, Budapest, Hungary.

[C31] Szabó M, Barsy B, Kocsis K, Jártó F, Mátyás F (2018): Asszociatív félelmi tanulás különböző fázisainak thalamikus szabályozása. Poster, Magyar Tudomány Ünnepe, Budapest, Hungary.

[C32] Magyar A*, Kocsis K*, Kanti V, Babiczky Á, Varga K, Mátyás F (2017): Electrophysiological characterization of the lateral thalamoamygdalar pathway in a cell-type specific manner. Poster, Aspects of Neuroscience, Warsaw, Poland.

[C33] Barsy B*, Kocsis K*, Magyar A, Babiczky A, Kanti V, Varga K, Hillier D, Yizhar O, Acsády L, Mátyás F (2017): Anatomical and functional dissection of the thalamic amygdalar networks. Poster, Amygdala Function in Emotion, Cognition & Disease Gordon Research Conference, Easton, MA, U.S.

[C34] Babiczky, Á, Vivien K, Magyar A, Porrero C, Kocsis K, García-Amado M, Hillier D, Yizhar O, Clascá F, Mátyás F (2017): The forebrain circuits of auditory fear conditioning: diversity and specificity of thalamo-amygdaloid pathways in the mouse. Poster, FENS Regional Meeting, Pécs, Hungary.

[C35] Barsy B*, Kocsis K*, Magyar A, Kanti V, Babiczky Á, Földes TA, Varga K, Mátyás F (2017): Anatomical and functional dissection of the thalamo-amygdala circuitry underlying associative learning. Poster, FENS Regional Meeting, Pécs, Hungary.

[C36] Magyar A*, Kocsis K*, Kanti V, Babiczky Á, Varga K, Mátyás F (2017): Electrophysiological characterization of the lateral thalamoamygdalar pathway in a cell-type specific manner. Poster, FENS Regional Meeting, Pécs, Hungary.

[C37] Magyar A*, Kocsis K*, Kanti V, Babiczky Á, Varga K, Mátyás F (2017): Electrophysiological characterization of the lateral thalamoamygdalar pathway in a cell-type specific manner. Poster, HuNDoC, Pécs, Hungary.

Selected references

Alföldi P, Rubicsek G, Cserni G & Obál F (1990). Brain and core temperatures and peripheral vasomotion during sleep and wakefulness at various ambient temperatures in the rat. *Pflugers Arch* **417,** 336–341.

Barsy B, Kocsis K, Magyar A, Babiczky Á, Szabó M, Veres JM, Hillier D, Ulbert I, Yizhar O & Mátyás F (2020). Associative and plastic thalamic signaling to the lateral amygdala controls fear behavior. *Nat Neurosci* **23,** 625–637.

Bartlett EL (2013). The organization and physiology of the auditory thalamus and its role in processing acoustic features important for speech perception. *Brain Lang* **126,** 29–48.

Blasiak T, Zawadzki A & Lewandowski MH (2013). Infra-Slow Oscillation (ISO) of the Pupil Size of Urethane-Anaesthetised Rats ed. Dickson CT. *PLoS One* **8,** e62430.

Bordi F & LeDoux JE (1994). Response properties of single units in areas of rat auditory thalamus that project to the amygdala - I. Acoustic discharge patterns and frequency receptive fields. *Exp Brain Res* **98,** 261–274.

Clement EA, Richard A, Thwaites M, Ailon J, Peters S & Dickson CT (2008). Cyclic and sleep-like spontaneous alternations of brain state under urethane anaesthesia. *PLoS One* **3,** e2004.

Collins KJ, Exton-Smith AN & Dore C (1981). Urban hypothermia: preferred temperature and thermal perception in old age. *BMJ* **282,** 175–177.

Csernai M, Borbély S, Kocsis K, Burka D, Fekete Z, Balogh V, Káli S, Emri Z & Barthó P (2019). Dynamics of sleep oscillations is coupled to brain temperature on multiple scales. *J Physiol* **597,** 4069–4086.

Cservenak M, Keller D, Kis V, Fazekas EA, Ollos H, Leko AH, Szabo ER, Renner E, Usdin TB, Palkovits M & Dobolyi A (2017). A thalamo-hypothalamic pathway that activates oxytocin neurons in social contexts in female rats. *Endocrinology* **158,** 335–348.

Deboer T & Tobler I (1995). Temperature dependence of EEG frequencies during natural hypothermia. *Brain Res* **670,** 153–156.

Dijk DJ & Czeisler C a (1995). Contribution of the circadian pacemaker and the sleep homeostat to sleep propensity, sleep structure, electroencephalographic slow waves, and sleep spindle activity in humans. *J Neurosci* **15,** 3526–3538.

Driver HS, Dijk DJ, Werth E, Biedermann K & Borbely AA (1996). Sleep and the sleep electroencephalogram across the menstrual cycle in young healthy women. *J Clin Endocrinol Metab* **81,** 728–735.

Fekete Z, Csernai M, Kocsis K, Horváth ÁC, Pongrácz A & Barthó P (2017). Simultaneous in vivo recording of local brain temperature and electrophysiological signals with a novel neural probe. *J Neural Eng* **14,** 034001.

Fernandez LMJ & Lüthi A (2020). Sleep spindles: Mechanisms and functions. *Physiol Rev* **100,** 805–868.

Gründemann J (2021). Distributed coding in auditory thalamus and basolateral amygdala upon associative fear learning. *Curr Opin Neurobiol* **67,** 183–189.

Hayashi H, Sumino R & Sessle BJ (1984). Functional organization of trigeminal subnucleus interpolaris: nociceptive and innocuous afferent inputs, projections to thalamus, cerebellum, and spinal cord, and descending modulation from periaqueductal gray. *J Neurophysiol* **51,** 890–905.

Hayward J & Baker M (1969). A comparative study of the role of the cerebral arterial blood in the regulation of brain temperature in five mammals. *Brain Res* **16,** 417–440.

Kawamura H & Sawyer CH (1965). Elevation in brain temperature during paradoxical sleep. *Science* **150,** 912–913.

Komura Y, Tamura R, Uwano T, Nishijo H & Ono T (2005). Auditory thalamus integrates visual inputs into behavioral gains. *Nat Neurosci* **8,** 1203–1209.

Kovalzon VM (1973). Brain temperature variations during natural sleep and arousal in white rats. *Physiol Behav* **10,** 667–670.

Krauchi K & Deboer T (2010). The interrelationship between sleep regulation and thermoregulation. *Front Biosci (Landmark Ed* **15,** 604–625.

LaManna JC, McCracken KA, Patil M & Prohaska OJ (1989). Stimulus-activated changes in brain tissue temperature in the anesthetized rat. *Metab Brain Dis* **4,** 225–237.

Lecci S, Fernandez LMJ, Weber FD, Cardis R, Chatton J-Y, Born J & Lüthi A (2017). Coordinated infraslow neural and cardiac oscillations mark fragility and offline periods in mammalian sleep. *Sci Adv* **3,** e1602026.

LeDoux JE, Farb C & Ruggiero D a (1990). Topographic organization of neurons in the acoustic thalamus that project to the amygdala. *J Neurosci* **10,** 1043–1054.

LeDoux JE, Sakaguchi A & Reis DJ (1984). Subcortical efferent projections of the medial geniculate nucleus mediate emotional responses conditioned to acoustic stimuli. *J Neurosci* **4,** 683–698.

Linke R, De Lima AD, Schwegler H & Pape HC (1999). Direct synaptic connections of axons from superior colliculus with identified thalamo-amygdaloid projection neurons in the rat: possible substrates of a subcortical visual pathway to the amygdala. *J Comp Neurol* **403,** 158–170.

Lipshetz B, Khasabov SG, Truong H, Netoff TI, Simone DA & Giesler GJ (2018). Responses of thalamic

neurons to itch- and pain-producing stimuli in rats. *J Neurophysiol* **120,** 1119–1134.
Lopes G, Bonacchi N, Frazão J, Neto JP, Atallah B V., Soares S, Moreira L, Matias S, Itskov PM, Correia PA, Medina RE, Calcaterra L, Dreosti E, Paton JJ & Kampff AR (2015). Bonsai: an event-based framework for processing and controlling data streams. *Front Neuroinform* **9,** 7.
Lőrincz ML, Geall F, Bao Y, Crunelli V & Hughes SW (2009). ATP-dependent infra-slow (<0.1 Hz) oscillations in thalamic networks. *PloS One* **4,** e4447.
Lyamin OI, Kosenko PO, Korneva SM, Vyssotski AL, Mukhametov LM & Siegel JM (2018). Fur Seals Suppress REM Sleep for Very Long Periods without Subsequent Rebound. *Curr Biol*1–6.
Malkinson TJ, Cooper KE & Veale WL (1988). Physiological changes during thermoregulation and fever in urethan-anesthetized rats. *Am J Physiol Integr Comp Physiol* **255,** R73–R81.
Mantini D, Perrucci MG, Del Gratta C, Romani GL & Corbetta M (2007). Electrophysiological signatures of resting state networks in the human brain. *Proc Natl Acad Sci* **104,** 13170–13175.
Nabavi S, Fox R, Proulx CD, Lin JY, Tsien RY & Malinow R (2014). Engineering a memory with LTD and LTP. *Nature* **511,** 348–352.
Parri HR & Crunelli V (2001). Pacemaker calcium oscillations in thalamic astrocytes *in situ*. *Neuroreport* **12,** 3897–3900.
Pouille F & Scanziani M (2001). Enforcement of temporal fidelity in pyramidal cells by somatic feed-forward inhibition. *Science (80-)* **293,** 1159–1163.
Raymann RJEM, Swaab DF & Van Someren EJW (2008). Skin deep: Enhanced sleep depth by cutaneous temperature manipulation. *Brain* **131,** 500–513.
Rosanova M & Ulrich D (2005). Pattern-specific associative long-term potentiation induced by a sleep spindle-related spike train. *J Neurosci* **25,** 9398–9405.
Rossant C, Kadir SN, Goodman DFM, Schulman J, Hunter MLD, Saleem AB, Grosmark A, Belluscio M, Denfield GH, Ecker AS, Tolias AS, Solomon S, Buzsáki G, Carandini M & Harris KD (2016). Spike sorting for large, dense electrode arrays. *Nat Neurosci* **19,** 634–641.
Van Someren EJW (2000). More Than a Marker: Interaction Between the Circadian Regulation of Temperature and Sleep, Age-Related Changes, and Treatment Possibilities. *Chronobiol Int* **17,** 313–354.
Van Someren EJW (2004). Sleep propensity is modulated by circadian and behavior-induced changes in cutaneous temperature. *J Therm Biol* **29,** 437–444.
Stein BE & Dixon JP (1978). Superior colliculus cells respond to noxious stimuli. *Brain Res* **158,** 65–73.
Steriade M, Deschenes M, Domich L & Mulle C (1985). Abolition of spindle oscillations in thalamic neurons disconnected from nucleus reticularis thalami. *J Neurophysiol* **54,** 1473–1497.
Steriade M, McCormick DA & Sejnowski TJ (1993). Thalamocortical oscillations in the sleeping and aroused brain. *Science* **262,** 679–685.
Sund-Levander M, Forsberg C & Wahren LK (2002). Normal oral, rectal, tympanic and axillary body temperature in adult men and women: a systematic literature review. *Scand J Caring Sci* **16,** 122–128.
Tang LS, Taylor AL, Rinberg A & Marder E (2012). Robustness of a Rhythmic Circuit to Short- and Long-Term Temperature Changes. *J Neurosci* **32,** 10075–10085.
Tasaka G ichi, Feigin L, Maor I, Groysman M, DeNardo LA, Schiavo JK, Froemke RC, Luo L & Mizrahi A (2020). The Temporal Association Cortex Plays a Key Role in Auditory-Driven Maternal Plasticity. *Neuron* **107,** 566-579.e7.
Wang H, Wang B, Normoyle KP, Jackson K, Spitler K, Sharrock M, Miller CM, Best C, Llano D & Du R (2014). Brain temperature and its fundamental properties: A review for clinical neuroscientists. *Front Neurosci* **8,** 1–17.
Weinberger NM (2011). The medial geniculate, not the amygdala, as the root of auditory fear conditioning. *Hear Res* **274,** 61–74.
Whitten T a, Martz LJ, Guico A, Gervais N & Dickson CT (2009). Heat synch: inter- and independence of body-temperature fluctuations and brain-state alternations in urethane-anesthetized rats. *J Neurophysiol* **102,** 1647–1656.